Glucose-regulated *O*-GlcNAcylation of DNMT1 inhibits DNA methyltransferase activity and maintenance of genomic methylation

Heon Shin[1], Amy Leung[1], Kevin R. Costello[1,2], Parijat Senapati[1], Hiroyuki Kato[1], Dustin E. Schones[1,2,3]*

[1]Department of Diabetes Complications and Metabolism, Beckman Research Institute, City of Hope, Duarte, California 91010 USA

[2]Irell and Manella Graduate School of Biological Sciences, City of Hope, Duarte, California 91010 USA

[3]Lead Contact

*Correspondence: dschones@coh.org

SUMMARY

The production of *O*-GlcNAc for protein *O*-GlcNAcylation is highly tuned to the metabolic state of the cell and thus can serve as a nutrient sensor responding to changes in metabolic pathways. We report here that excess glucose leads to increased *O*-GlcNAcylation of DNMT1, resulting in inhibition of DNA methyltransferase 1 (DNMT1) function and alterations to the epigenome. Using mass spectrometry and complementary alanine mutation experiments, we identified S878 as the major residue that is *O*-GlcNAcylated on DNMT1. Functional studies reveal that *O*-GlcNAcylation of DNMT1-S878 reduces its DNA methyltransferase activity. Treatment of cells with prolonged high glucose induces loss of DNA methylation, preferentially at partially methylated domains (PMDs). We further find that the high glucose-induced DNA methylation loss is attenuated in cells expressing DNMT1-S878A. These results establish *O*-GlcNAcylation of DNMT1 as a mechanism through which the epigenome is regulated by glucose metabolism and implicates a role for glycosylation of DNMT1 in metabolic diseases characterized by hyperglycemia.

INTRODUCTION

Excess glucose, or hyperglycemia, is a hallmark of obesity and the defining clinical feature of diabetes (American Diabetes Association, 2009). Metabolically, hyperglycemia leads to cellular glucose uptake which, in turn, increases flux of glucose utilization pathways and production of metabolites (Hawkins et al., 1997; Herman and Kahn, 2006). One downstream output of glucose metabolism is the nucleotide sugar, UDP-GlcNAc,

that is used as a substrate for protein *O*-GlcNAcylation (Hawkins et al., 1997; Slawson et al., 2010).

Protein *O*-GlcNAcylation is a dynamic and reversible post-translational modification that attaches a single *O*-linked β-*N*-acetylglucosamine to serine or threonine residues (Hart et al., 1996). It is modulated by two *O*-GlcNAc cycling enzymes, *O*-GlcNAc transferase (OGT) (O'Donnell et al., 2004; Shafi et al., 2000) and *O*-GlcNAcase (OGA) (Yang et al., 2012) depending on nutritional status (Hart et al., 2007; Slawson et al., 2010). The increased concentration of UDP-GlcNAc that is observed in conditions of excess glucose leads to increased protein *O*-GlcNAcylation (Hart, 2006; Walgren et al., 2003). Obesogenic diets have been shown to have elevated protein *O*-GlcNAcylation in various human cell types, including the liver (Guinez et al., 2011), lymphocytes (Torres and Hart, 1984), and immune cells (de Jesus et al., 2018).

As with other post-translational modifications, *O*-GlcNAcylation of proteins can influence the function and/or stability of the targeted proteins (Hart et al., 2011; Hayes and Hart, 1998; Shin et al., 2018; Yang and Qian, 2017). Thousands of proteins are targets for *O*-GlcNAcylation, including many epigenetic regulatory proteins. For example, the *O*-GlcNAcylation of TET family proteins impacts their activity, localization and targeting (Chen et al., 2013; Ito et al., 2014; Shi et al., 2013; Zhang et al., 2014). All DNA methyltransferases have furthermore been shown to be *O*-GlcNAcylated, although the functional consequences of this are unclear (Boulard et al., 2020).

Among the DNA methyltransferase (DNMT) family of proteins, DNMT1 is imperative for maintaining DNA methylation patterns in replication (Bestor and Ingram, 1983). DNMT1 is a modular protein with several domains necessary for interacting with

cofactors, including the BAH1 and BAH2 domains (Maresca et al., 2015; Ren et al., 2018). The stability and function of DNMT1 has been shown to be regulated through post-translational modifications including acetylation, phosphorylation, and methylation (Scott et al., 2014).

Partially methylated domains, large domains with a loss of DNA methylation, were originally identified in cultured cell lines (Lister et al., 2009) and subsequently found to be a characteristic of cancer cells (Berman et al., 2011; Brinkman et al., 2019). PMDs have also been detected in non-cancerous healthy tissues, where they are associated with late replication loci (Hansen et al., 2010; Zhou et al., 2018). While PMDs are generally thought to arise from a lack of fidelity in maintenance methylation (Decato et al., 2020), the mechanisms responsible for the establishment of PMDs have remained unclear. Here, we report that the activity of DNMT1 is regulated by extracellular levels of glucose through its *O*-GlcNAcylation resulting in loss of methylation at PMDs.

RESULTS

High glucose conditions increase *O*-GlcNAcylation of DNMT1

To validate that DNMT1 can be *O*-GlcNAcylated, we treated Hep3B cells with OSMI-4 (OSMI), an OGT inhibitor (Martin et al., 2018), as well as with Thiamet-G (TMG), an OGA inhibitor (Elbatrawy et al., 2020). As expected, immunoblots of cellular lysate with an antibody recognizing pan-*O*-GlcNAc (RL2) reveal that inhibition of OGA increased global levels of *O*-GlcNAc while inhibition of OGT decreased global levels of *O*-GlcNAc (**Figure S1**A). To distinguish whether DNMT1 is *O*-GlcNAcylated, immunoprecipitates from the cellular lysates treated with OSMI or TMG were generated with DNMT1 antibodies.

Immunoblots with *O*-GlcNAc antibodies reveal that TMG treatment increases *O*-GlcNAc of DNMT1 while OSMI treatment decreases *O*-GlcNAc (**Figure S1**B). In addition to Hep3B cells, we found that DNMT1 is *O*-GlcNAcylated in HepG2 cells and B cell derived lymphocytes, indicating DNMT1 is *O*-GlcNAcylated across various cell types (**Figures S1**C and S1D).

To assess the effect of increased glucose metabolism on *O*-GlcNAcylation of DNMT1, we treated Hep3B cells with glucose or sucrose (5mM or 25mM) and examined global protein *O*-GlcNAcylation as well as the *O*-GlcNAcylation of DNMT1 specifically. Consistent with previous reports (Andrews et al., 2000), the total amount of protein *O*-GlcNAcylation was increased with 25mM of glucose (**Figure 1**A). Global protein *O*-GlcNAcylation was also induced with 25mM sucrose, albeit to a lower extent than with glucose (**Figure 1**A). To specifically assess the level of *O*-GlcNAcylated DNMT1, we performed immunoprecipitation of DNMT1 from lysates of glucose treated Hep3B cells and immunoblotted for *O*-GlcNAc. As with the analysis of total protein, high glucose treatment (25mM) increased the expression of *O*-GlcNAcylation of DNMT1 (**Figures 1**B and **S1**E). To examine whether an increase of *O*-GlcNAcylation of DNMT1 also occurs in primary cells, we collected peripheral blood mononuclear cells (PBMCs) from three separate donors and treated the PBMCs with increasing glucose levels (0mM, 5mM, 10mM, 15mM, and 20mM). Similar to our observations in Hep3B cells, we observed an increase in *O*-GlcNAcylation of DNMT1 with increased glucose (**Figures 1**C and 1D). These data validate the *O*-GlcNAcylation of DNMT1 and that the degree of modification of DNMT1 increases with glucose concentrations.

Identification of the major *O*-GlcNAcylation sites of DNMT1

To begin to identify the major residues *O*-GlcNAcylated on DNMT1 we utilized OGTsite (http://csb.cse.yzu.edu.tw/OGTSite/index.php) (Kao et al., 2015) to predict potential sites of *O*-GlcNAcylation. OGTsite, which uses experimentally verified *O*-GlcNAcylation sites to build models of substrate motifs, identified 22 candidate *O*-GlcNAc modified sites on human DNMT1 (**Table S1)**. We next employed mass spectrometry analysis to examine the post-translational modifications on DMNT1 in Hep3B cells. We generated a construct with Myc-tagged DNMT1 to increase the level of expressed DNMT1. Immunoblots with Myc antibody (Yompakdee et al., 1996) revealed a band corresponding to Myc-DNMT1 in transfected, but not mock transfected, cells (**Figure S2**A). We further confirmed with immunoprecipitation followed by immunoblot that the overexpressed Myc-DNMT1 can be *O*-GlcNAcylated (**Figure S2**B). For mass spectrometry analysis, we treated Myc-DNMT1 expressing cells with 25mM Thiamet-G (TMG) to further increase the *O*-GlcNAcylation of DNMT1. Myc-DNMT1 was enriched from transfected cells by monoclonal Ab-crosslinked immunoprecipitation and subjected to in-solution digestion using three different enzymes (AspN, chymotrypsin, and LysC) and high-resolution LC-MS/MS analysis. Peptide analyses revealed that S878, which is located on the bromo-associated homology (BAH1) domain of the DNMT1 is *O*-GlcNAcylated (**Figures 2**A, 2B, and **S2**C; **Table S2**). In addition, eight unreported phosphorylated residues were newly detected (T208, S209, S873, S874, S953, S954, S1005, and S1202) (**Table S2**).

We chose the three top candidates based on prediction score (T158, T616, and T882) as well as the site identified from mass spectrometry analysis (S878) for further analysis with alanine mutation experiments. The threonine/serine residues were mutated

to alanine residues on our Myc-DNMT1 construct and *O*-GlcNAcylation was evaluated with immunoblot following immunoprecipitation. Loss of threonine and serine at positions T158 and S878 respectively resulted in a loss of *O*-GlcNAcylation, indicating that these two residues are required for *O*-GlcNAcylation, with the DNMT1-S878A mutant resulting in > 50% reduction of *O*-GlcNAcylation (**Figure 2**C). These results indicate that T158 (near the PCNA binding domain) and S878 (within the BAH1 domain) are the DNMT1 residues modified with *O*-GlcNAcylation.

O-GlcNAcylation of DNMT1 results in loss of DNA methyltransferase activity

The BAH domains of DNMT1 have been found to be necessary for DNA methyltransferase activity (Yarychkivska et al., 2018). Given that S878 is in the BAH1 domain, we reasoned that *O*-GlcNAcylation of this residue could impact the DNA methyltransferase activity of DNMT1. To test this, we treated Hep3B cells with either 5mM or 25mM of glucose as well as with 25 mM Thiamet-G (TMG) or DMSO as control and evaluated the DNA methyltransferase activity of immunoprecipitated DNMT1 with the EpiQuik DNMT Activity/Inhibition ELISA Easy Kit (EpiGentek, details in STAR Methods). Intriguingly, high glucose (25mM) treatment reduced the activity of DNMT1 and additional treatment of cells with TMG further inhibited the activity of DNMT1 (**Figures 3**A and **S3**A).

To examine whether elevated glucose affected the function of DNMT1 in primary cells, we treated PBMCs with increasing concentrations of glucose (0mM, 5mM, 10mM, 15mM, 20mM and 25mM with Thiamet-G) for 96 hours and analyzed the DNA methyltransferase activity of DNMT1. We observed a striking dose-dependent inhibition of the DNA methyltransferase activity of DNMT1 (**Figures 3**B and 3C). Together, these

data indicate that elevated levels of extracellular glucose can inhibit the methyltransferase function of DNMT1.

We next examined the ability of the DNMT1 alanine mutants (DNMT1-T158A and DNMT1-S878A) to attenuate the impact of high glucose- and TMG-induced loss of DNA methyltransferase activity. Compared to the DNA methyltransferase activity of DNMT1-WT (Myc-DNMT1-WT), which is sensitive to high glucose/TMG treatment, the DNA methyltransferase activity of Myc-DNMT1-S878A is not inhibited by high glucose treatment (**Figure 3**D). In contrast, the DNA methyltransferase activity of Myc-DNMT1-T158A is inhibited by high glucose/TMG treatment in a manner similar to DNMT1-WT, indicating that *O*-GlcNAcylation of DNMT1-T158 does not affect its DNA methyltransferase activity.

A previous phosphoproteomic analysis revealed that DNMT1-S878 can be phosphorylated (Zhou et al., 2013). To evaluate the potential that phosphorylation, rather than *O*-GlcNAcylation, of S878 is leading to the loss of DNA methyltransferase activity, we generated Myc-DNMT1-S878D, a phosphomimetic mutant that cannot be *O*-GlcNAcylated, and examined DNA methyltransferase activity in normal and high glucose conditions. This phosphomimetic mutant did not have loss of DNA methyltransferase activity under high glucose conditions, indicating that *O*-GlcNAcylation of S878 but not phosphorylation of S878 is leading to loss of methyltransferase activity of DNMT1 (**Figure 3**D).

O-GlcNAcylation of DNMT1 results in subsequent loss of DNA methylation

Given our observations that *O*-GlcNAcylation of DNMT1 under high glucose/TMG inhibits its DNA methyltransferase activity, we reasoned that these conditions would result in a general loss of DNA methylation. To assess this, DNA methylation was assayed using the global DNA methylation LINE-1 kit (Active Motif, details in STAR Methods) as a proxy for global methylation. Comparison of DNA methylation levels under high glucose and TMG with a DNA methylation inhibitor (5-aza; details in STAR Methods) revealed that high glucose leads to a loss of DNA methylation in a manner comparable with the DNA methylation inhibitor (**Figure 3**E). This methylation loss was not apparent in the Myc-DNMT1-S878A mutant, further demonstrating that *O*-GlcNAcylation of S878 serine within DNMT1 directly affects DNA methylation under high glucose conditions (**Figures 3**E and **S3**B). A complementary assessment of DNA methylation using methylation sensitive restriction enzymes and gel electrophoresis (details in STAR Methods) revealed similar trends (**Figure S3**C).

O-GlcNAcylation of DNMT1 results in loss of DNA methylation at partially methylated domains (PMDs)

To further examine alterations to DNA methylation upon high glucose induced *O*-GlcNAcylation of DNMT1, we performed genomic methylation profiling with nanopore sequencing (ONT PromethION; details in STAR Methods). The Myc-DNMT1 overexpressed cell lines (Myc-DNMT1-WT and Myc-DNMT1-S878A) were treated with TMG and either 5mM or 25mM glucose and DNA methylation was profiled in duplicate. Considering only CpGs with > 5x coverage (**Figure S4**A), we observed a global loss of methylation in the high glucose/TMG treatment compared to control (**Figures 4**A, 4B and

S4B-S4G). Conversely, for the DNMT1-S878A mutant, there was no appreciable decrease in DNA methylation by high glucose/TMG treatment (**Figure 4**A). These results collectively indicate that *O*-GlcNAcylation of S878 of DNMT1 leads to a global loss of DNA methylation.

Examination of DNA methylation changes induced by *O*-GlcNAcylation of DNMT1 revealed a preferential loss of DNA methylation at liver cancer PMDs (Li et al., 2016) that was not observed in S878A mutant cells (**Figures 4**B and 4C). Partially methylated domains (PMDs) have several defining features, including being relatively gene poor and harboring mostly lowly transcribed genes (Decato et al., 2020). We stratified the genome in terms of gene density and transcription rate (see STAR Methods for details) and found that regions that lose methylation in high glucose conditions are largely gene poor (**Figure 4**D) and contain lowly transcribed genes (**Figure S4**H) (Chang et al., 2014). PMDs have furthermore been linked to regions of late replication associated with the nuclear lamina (Brinkman et al., 2019). We therefore examined the correlation between loss of methylation caused by high glucose/TMG and replication timing (Thurman et al., 2007). In DNMT1-WT cells, late replication domains preferentially lose DNA methylation in high glucose/TMG conditions compared to early replication domains (**Figure 4**E). This loss of methylation was not observed in S878A mutant cells (**Figure S4**I).

It has previously been demonstrated that certain genes within PMDs “escapee” the general loss of methylation and reduced expression observed in PMDs (Decato et al., 2020). We found 270 genes within PMDs that retained methylation and transcription signatures in high glucose conditions, including 147 that overlap with other cell types (Decato et al., 2020) (**Figure S4**J).

One of the major functions of DNA methylation in mammalian genomes is the repression of repetitive elements (Edwards et al., 2017). It has furthermore been shown that many chromatin proteins involved in the repression of transposable elements (TEs) are capable of being *O*-GlcNAcylated (Boulard et al., 2020). We therefore examined the potential of *O*-GlcNAcylation of DNMT1 to lead to loss of suppression of TEs. We found that high glucose conditions resulted in methylation loss at TEs in a manner similar to the non-repetitive fraction of the genome (**Figure S5**A), with a more dramatic loss of methylation at LINEs and LTRs as compared to SINE elements (**Figures S5**B-S5D). Given that evolutionarily recent TEs are more likely to lose methylation than older elements in a variety of systems (Almeida et al., 2022; Zhou et al., 2020), we examined the methylation status of two younger subfamilies, LTR12C (*Hominoidea*) and HERVH-int (*Catarrhini*) elements (**Figure S5**E). While HERVH-int elements show a loss of methylation similar to the rest of the genome, LTR12C elements do not lose methylation in the same manner (**Figures S5**E and S5F) suggesting they are protected from the loss of methylation. Stratifying all TEs by evolutionary age and examining the methylation changes induced by *O*-GlcNAcylation of DNMT1 for each clade revealed that evolutionarily recent elements are less likely to lose methylation (**Figure S**5G).

DISCUSSION

Although there is a great deal of evidence regarding the important regulatory role of *O*-GlcNAcylation in gene regulation (Brimble et al., 2010), a direct link with DNA methylation has not previously been established. The maintenance methyltransferase DNMT1 is essential for faithful maintenance of genomic methylation patterns and mutations in

DNMT1, particularly in the BAH domains, lead to disruption of DNA methylation (Yarychkivska et al., 2018). While it has been shown that DNTM1 can be *O*-GlcNAcylated (Boulard et al., 2020), the site of *O*-GlcNAc modification on DNMT1 as well as the functional consequences of this modification have not previously been examined.

We reveal that *O*-GlcNAcylation of DNMT1 impacts its DNA methyltransferase activity and affects DNMT1 function leading to loss of DNA methylation at PMDs. PMDs are observed in both healthy and cancerous cells and have been suggested to be associated with mitotic dysfunction. However, models for how these domains are established remain incomplete (Decato et al., 2020). The results presented here suggest an additional layer whereby *O*-GlcNAcylation of DNMT1 at S878 due to increased glucose levels can inhibit the function of DNA methyltransferase activity of DNMT1, resulting in loss of methylation and establishment of partially methylated domains.

Metabolic diseases such as obesity and diabetes have been linked to epigenetic changes that alter gene regulation (Al-Haddad et al., 2016; Dalgaard et al., 2016; Ling and Ronn, 2019). It has previously been established that there is a general increase in protein *O*-GlcNAcylation in hyperglycemia conditions (Vasconcelos-Dos-Santos et al., 2018) and several epigenetic regulatory factors have been shown to have increased *O*-GlcNAcylation under high glucose conditions (Bauer et al., 2015; Etchegaray and Mostoslavsky, 2016; Yang et al., 2020). Our findings that extracellular glucose promotes *O*-GlcNAcylation of DNMT1 and inhibition of DNMT1's function in maintenance of genomic methylation provide direct evidence that extracellular levels of glucose is linked with epigenomic regulation.

ACKNOWLEDGEMENTS

This manuscript is dedicated to the memory of the exceptional and brilliant scientist Dr. Arthur Riggs. This work was supported by the National Institutes of Health, grants R01DK112041 and R01CA220693 (D.E.S.). Research reported in this publication included work performed in the Pathology and Integrative Genomics Cores of the City of Hope and was supported by the City of Hope CCSG Pilot award from National Cancer Institute of the National Institutes of Health under award number P30CA033572.

AUTHOR CONTRIBUTION

Conceptualization, H.S., A.L., and D.E.S.; Methodology: H.S., A.L., and K.R.C.; Software: H.S., A.L., K.R.C., and P.S.; Validation: H.S.; Formal Analysis, H.S., A.L., K.R.C., and H.K.; Resources, H.S., A.L., K.R.C., P.S., and D.E.S.; Data Curation, H.S., A.L., and K.R.C.; Writing – Original Draft, H.S., and A.L.; Writing- Review & Editing, H.S., A.L., and D.E.S.; Visualization, H.S., and K.R.C; Supervision, A.L., and D.E.S.; Project Administration, A.L., and D.E.S.; Funding Acquisition, D.E.S.

DECLARATION OF INTERESTS

The authors declare that they have no conflicts of interest with the contents of this article. The content is solely the responsibility of the authors and does not necessarily represent the official views of the National Institutes of Health.

MAIN FIGURE TITLES AND LEGENDS

Figure 1. High glucose increases *O*-GlcNAcylation of DNMT1 in cell lines and primary cells.

(A) Hep3B cells were treated glucose or sucrose (5mM or 25mM). Shown are immunoblots of collected lysates using antibody targeting *O*-GlcNAc and GAPDH (n = 3).

(B) Lysates of Hep3B treated with glucose were immunoprecipitated with DNMT1 and immunoprecipitates were immunoblotted with antibody targeting *O*-GlcNAc (n = 3).

(C) PBMCs were isolated from three individual donor blood samples and treated with increasing concentration of glucose for 24 hours. Collected cell lysates from PBMCs were immunoprecipitated with antibody targeting DNMT1 and immunoblotted for *O*-GlcNAc. This is from one donor set. (n = 3).

(D) Pooled PBMCs treated with 25 mM glucose with Thiamet-G were immunoprecipitated with antibody targeting DNMT1 and immunoblotted for *O*-GlcNAc (n = 3).

***$p < 0.0001$ by Student's *t*-test (A-D); n.s., not significant; Data are represented as mean ± SD from three replicates of each sample.

Figure 2. Identification of *O*-GlcNAcylated sites within DNMT1 by LC-MS/MS.

(A) Schematic drawing of the DNMT1 *O*-GlcNAc modified region enriched from Hep3B cells based on mass spectrometry (MS) data and tandem MS (MS/MS) peaks. FTMS + p NSI Full MS [400.0000-1600.0000]. DQDYARFESPPKTQPTEDNKF (S9 HexNAc) – S878.

(B) Schematic diagram of identified novel *O*-GlcNAcylated sites within DNMT1 as determined via MS and OGTsite. DMAP, DNA methyltransferase associated protein-binding domain; PCNA, proliferating cell nuclear antigen-binding domain; NLS, nuclear localization sequences; RFTS, replication foci targeting sequence domain; BAH, bromo-adjacent homology domain.

(C) Each immunoprecipitated Myc-DNMT1 wild type and substituted mutants was immunoblotted with an *O*-GlcNAc antibody (n = 3).

Figure 3. Site specific *O*-GlcNAcylation inhibits DNMT1 methyltransferase function.

For (A)-(D), bar graphs are of relative activity of DNA methyltransferase activity measured as absorbance from of DNMT Activity/Inhibition ELISA easy kit and representative immunoblots of immunoprecipitates performed with antibodies targeting DNMT1.

(A) Hep3B cells were treated 5mM or 25mM glucose with or without TMG (n = 3).

(B) PBMCs from donors were treated with increasing concentrations of glucose (range: 0-20mM) (n = 3).

(C) PBMCs from donors were treated 5mM or 25mM glucose with TMG (n = 3).

(D) Each immunoprecipitated Myc-DNMT1 wild type and substituted mutants were treated with 5mM or 25mM glucose (n = 3).

(E) Each Hep3B and Myc-DNMT1 overexpressed mutants (DNMT1-WT or DNMT1-S878A) were treated 5mM or 25mM glucose or 5-aza (negative control). Shown are

absorbance of global DNA methylation of LINE-1 performed with global DNA methylation LINE-1 kit. (n = 3).
*$p < 0.001$; **$p < 0.005$; ***$p < 0.0001$ by Student's *t*-test (A-E); ns, not significant; Data are represented as mean ± SD from three replicates of each sample.

Figure 4. High glucose leads to loss of DNA methylation at cancer specific partially methylated domains (PMDs).
(A) Density plot of DNA methylation for DNMT1-WT and DNMT1-S878A cells and low or high glucose.
(B) Genome browser screenshot of DNA methylation for DNMT1-WT and DNMT1-S878A cells and low or high glucose along with liver tumor PMDs from (Li et al., 2016).
(C) Boxplots of DNA methylation at PMDs or general genomic background (BG) for each DNMT1-WT and DNMT1-S878A treated with low or high glucose.
(D) Heatmap representation of global DNA methylation for DNMT1-WT and DNMT1-S878A cells under low or high glucose at gene poor and gene rich regions.
(E) Methylation changes from *O*-GlcNAcylation of DNMT1 by wave score for replication timing (Hansen et al., 2010; Thurman et al., 2007).

STAR METHODS

Detailed methods are provided in the online version of this paper and include the following:

- KEY RESOURCES TABLE
- RESOURSE AVAILABILITY
  - Lead contact
  - Materials availability
  - Data and code availability
- EXPERIMENTAL MODEL AND SUBJECT DETAILS
  - Hepatocarcinoma cells (Hep3B and HepG2)
  - Peripheral blood mononuclear cell (PBMC)
  - Isolation of B cells and Epstein-Barr virus (EBV) infection for Lymphocytes transformation
- METHOD DETAILS
  - Immunoprecipitation and western blot analysis
  - Protein identification using the Thermo Fusion Lumos system LC-MS/MS
  - Site-directed point mutation
  - DNA methyltransferase activity assay
  - Global DNA Methylation LINE-1 assay
  - Agilent 4200 TapeStation
  - Nanopore PromethION sequencing
- QUANTIFICATION AND STATISTICAL ANALYSIS
  - Statistical analysis
- DATA AND SOFTWARE AVAILABILITY

SUPPLEMENTAL INFORMATION

Supplementary Figures

Figure S1. High glucose increases *O*-GlcNAcylation of DNMT1.
(A) Hep3B cells were treated with Thiamet-G (TMG) or OSMI-4 (OSMI). Shown are representative immunoblots of treated Hep3B lysates performed with antibodies targeting

O-GlcNAc, and GAPDH and bar graphs of relative expression between *O*-GlcNAc compared to control, GAPDH (n = 3, experimental replicates).
(B) Lysates from treated Hep3B with glucose were immunoprecipitated with DNMT1 and immunoprecipitates were immunoblotted with antibody targeting *O*-GlcNAc (n = 3).
(C) HepG2 cells were treated with Thiamet-G or OSMI. Shown are immunoblots of treated HepG2 lysates performed with immunoblots of immunoprecipitates performed with antibodies targeting *O*-GlcNAc.
(D) Shown are immunoblots of B cell and lymphocytes (LCL) lysates performed with immunoblots of immunoprecipitates performed with antibodies targeting *O*-GlcNAc.
(E) HepG2 cells were treated 5mM glucose or sucrose, or 25mM glucose or sucrose. Lysates of HepG2 treated with glucose were immunoprecipitated with DNMT1 and immunoprecipitates were immunoblotted with antibody targeting *O*-GlcNAc.
***$p < 0.0001$ by Student's *t*-test (A-E); Data are represented as mean ± SD from three replicates of each sample.

Figure S2. Myc-DNMT1-WT in Hep3B cells is *O*-GlcNAcylated.
(A) Myc-DNMT1-WT were transfected into Hep3B cells. Shown are immunoblots of treated DNMT1-WT lysates performed with antibodies targeting Myc, DNMT1, Tubulin, H3, and *O*-GlcNAc.
(B) Lysates from treated DNMT1-WT in (A) were immunoprecipitated with Myc antibody. Shown are immunoblots of immunoprecipitates performed with antibodies targeting *O*-GlcNAc and CBB stained gel.
(C) Tandem MS/MS peaks of *O*-GlcNAcylated DNMT1 peptides.

Figure S3. Site specific *O*-GlcNAcylation at DNMT1 sites abrogate the function of methyltransferase and DNA loss of methylation at CpG island under high glucose/TMG conditions.
(A) HepG2 cells were treated 5mM glucose, 25mM glucose with or without Thiamet-G (TMG). Shown are absorbance of DNA methyltransferase activity performed with DNA methyltransferase activity kit. (n = 3, technical replicates from 3 biological replicates for each strain).
(B) Each HepG2 and Myc-DNMT1 overexpressed mutants (DNMT1-WT or DNMT1-S878A) were treated 5mM glucose, or 25mM glucose, or 5-aza (negative control). Shown are absorbance of global DNA methylation of LINE-1 performed with global DNA methylation LINE-1 kit. (n = 3, technical replicates from 3 biological replicates for each strain).
(C) DNA was extracted from Hep3B and Myc-DNMT1 overexpressed mutants (DNMT1-WT or DNMT1-S878A) were treated 5mM glucose, or 25mM glucose, or 5-aza (negative control) with MspI (negative control) or HpaII. Shown are extracted genomic DNA

samples and analyze on the 4200 TapeStation System with the Genomic DNA Screen Tape assay with methylation sensitive enzyme using MspI or HpaII.
*p < 0.001; ***p < 0.0001 by Student's t-test (A and B); n.s., not significant; Data are represented as mean ± SD from three replicates of each sample.

Figure S4. DNA loss of methylation by increased global *O*-GlcNAcylation decreases.
(A) Shown are overall CpGs sites that detected with over 5x coverage DNA methylation analysis using Nanopore technology PromethION sequencer. Each condition is biological replicated.
For (B)-(F), bar graphs represent percentage of global DNA methylation of wild type and DNMT1 mutants (DNMT1-WT or DNMT1-S878A) which treated 5mM glucose, or 25mM glucose with Thiamet-G.
(B) 5'UTR, (C) Promoter, (D) Gene body, (E) 3'UTR, (F) Intergenic regions.
(G) Genome browser screenshot of DNA methylation data at a differentially methylated region by glucose concentration.
(H) Heatmap represent global DNA methylation of wild type and DNMT1 mutants between low FPKM regions and high FPKM regions (DNMT1-WT or DNMT1-S878A) which treated 5mM glucose, or 25mM glucose with Thiamet-G were determined by Nanopolish call methylation. These are defined 'low FPKM' as containing less than 25% of RPKM regions per Mb window, and 'high FPKM' as containing more than 75% of RPKM regions per Mb window.
(I) The distribution of each DNA methylation was divided by DNA replication timing.
(J) Stitched browser plot showing 4 most conserved escapee genes and their methylation state (*MINDY3*, *ZWINT*, *ALG10B*, and *MAP3K7*).

Figure S5. DNA loss of methylation by increased global *O*-GlcNAcylation decreases around the transposable elements (TEs) regions.
(A) Boxplot represents the levels of DNA methylation on the TE regions or non-TE regions of each Myc-DNMT1 overexpressed mutants (DNMT1-WT or DNMT1-S878A) were treated 5mM glucose, or 25mM glucose with Thiamet-G.
For (B)-(D), bar graphs represent percentage of global DNA methylation of wild type and DNMT1 mutants (DNMT1-WT or DNMT1-S878A) which treated 5mM glucose, or 25mM glucose with Thiamet-G.
(B) SINE, (C) LINE, (D) LTR regions.
(E) Shown are methylation density around LTR12C regions of each Myc-DNMT1 overexpressed mutants (DNMT1-WT or DNMT1-S878A) were treated 5mM glucose, or 25mM glucose with Thiamet-G.
(F) Genome browser screenshot of DNA methylation data promoter region of *KCNAB1* by glucose concentration.

(G) Boxplot represents the DNA methylation by clades of the human genome (*Homo sapiens* to *Haplorhini*).

Supplementary Tables

Table S1. Prediction of *O*-GlcNAcylated sites within DNMT1 using OGTsite
Table S2. List of total identified proteins

REFERENCES

Al-Haddad, R., Karnib, N., Assaad, R.A., Bilen, Y., Emmanuel, N., Ghanem, A., Younes, J., Zibara, V., Stephan, J.S., and Sleiman, S.F. (2016). Epigenetic changes in diabetes. Neurosci Lett *625*, 64-69.
Almeida, M.V., Vernaz, G., Putman, A.L.K., and Miska, E.A. (2022). Taming transposable elements in vertebrates: from epigenetic silencing to domestication. Trends Genet.
Andrews, S.R., Charnock, S.J., Lakey, J.H., Davies, G.J., Claeyssens, M., Nerinckx, W., Underwood, M., Sinnott, M.L., Warren, R.A., and Gilbert, H.J. (2000). Substrate specificity in glycoside hydrolase family 10. Tyrosine 87 and leucine 314 play a pivotal role in discriminating between glucose and xylose binding in the proximal active site of Pseudomonas cellulosa xylanase 10A. J Biol Chem *275*, 23027-23033.
American Diabetes Association. (2009). Diagnosis and classification of diabetes mellitus. Diabetes care *32 Suppl 1*, S62-67.
Bauer, C., Gobel, K., Nagaraj, N., Colantuoni, C., Wang, M., Muller, U., Kremmer, E., Rottach, A., and Leonhardt, H. (2015). Phosphorylation of TET proteins is regulated via O-GlcNAcylation by the O-linked N-acetylglucosamine transferase (OGT). The Journal of biological chemistry *290*, 4801-4812.
Berman, B.P., Weisenberger, D.J., Aman, J.F., Hinoue, T., Ramjan, Z., Liu, Y., Noushmehr, H., Lange, C.P., van Dijk, C.M., Tollenaar, R.A., et al. (2011). Regions of focal DNA hypermethylation and long-range hypomethylation in colorectal cancer coincide with nuclear lamina-associated domains. Nat Genet *44*, 40-46.
Bestor, T.H., and Ingram, V.M. (1983). Two DNA methyltransferases from murine erythroleukemia cells: purification, sequence specificity, and mode of interaction with DNA. Proc Natl Acad Sci U S A *80*, 5559-5563.
Boulard, M., Rucli, S., Edwards, J.R., and Bestor, T.H. (2020). Methylation-directed glycosylation of chromatin factors represses retrotransposon promoters. Proceedings of the National Academy of Sciences of the United States of America *117*, 14292-14298.
Brimble, S., Wollaston-Hayden, E.E., Teo, C.F., Morris, A.C., and Wells, L. (2010). The Role of the O-GlcNAc Modification in Regulating Eukaryotic Gene Expression. Curr Signal Transduct Ther *5*, 12-24.
Brinkman, A.B., Nik-Zainal, S., Simmer, F., Rodriguez-Gonzalez, F.G., Smid, M., Alexandrov, L.B., Butler, A., Martin, S., Davies, H., Glodzik, D., et al. (2019). Partially methylated domains are hypervariable in breast cancer and fuel widespread CpG island hypermethylation. Nat Commun *10*, 1749.

Chang, C., Li, L., Zhang, C., Wu, S., Guo, K., Zi, J., Chen, Z., Jiang, J., Ma, J., Yu, Q., et al. (2014). Systematic analyses of the transcriptome, translatome, and proteome provide a global view and potential strategy for the C-HPP. J Proteome Res *13*, 38-49.
Chen, Q., Chen, Y., Bian, C., Fujiki, R., and Yu, X. (2013). TET2 promotes histone O-GlcNAcylation during gene transcription. Nature *493*, 561-564.
Dalgaard, K., Landgraf, K., Heyne, S., Lempradl, A., Longinotto, J., Gossens, K., Ruf, M., Orthofer, M., Strogantsev, R., Selvaraj, M., et al. (2016). Trim28 Haploinsufficiency Triggers Bi-stable Epigenetic Obesity. Cell *164*, 353-364.
de Jesus, T., Shukla, S., and Ramakrishnan, P. (2018). Too sweet to resist: Control of immune cell function by O-GlcNAcylation. Cell Immunol *333*, 85-92.
Decato, B.E., Qu, J., Ji, X., Wagenblast, E., Knott, S.R.V., Hannon, G.J., and Smith, A.D. (2020). Characterization of universal features of partially methylated domains across tissues and species. Epigenetics Chromatin *13*, 39.
Edwards, J.R., Yarychkivska, O., Boulard, M., and Bestor, T.H. (2017). DNA methylation and DNA methyltransferases. Epigenetics Chromatin *10*, 23.
Elbatrawy, A.A., Kim, E.J., and Nam, G. (2020). O-GlcNAcase: Emerging Mechanism, Substrate Recognition and Small-Molecule Inhibitors. ChemMedChem *15*, 1244-1257.
Etchegaray, J.P., and Mostoslavsky, R. (2016). Interplay between Metabolism and Epigenetics: A Nuclear Adaptation to Environmental Changes. Molecular cell *62*, 695-711.
Guinez, C., Filhoulaud, G., Rayah-Benhamed, F., Marmier, S., Dubuquoy, C., Dentin, R., Moldes, M., Burnol, A.F., Yang, X., Lefebvre, T., et al. (2011). O-GlcNAcylation increases ChREBP protein content and transcriptional activity in the liver. Diabetes *60*, 1399-1413.
Hansen, R.S., Thomas, S., Sandstrom, R., Canfield, T.K., Thurman, R.E., Weaver, M., Dorschner, M.O., Gartler, S.M., and Stamatoyannopoulos, J.A. (2010). Sequencing newly replicated DNA reveals widespread plasticity in human replication timing. Proc Natl Acad Sci U S A *107*, 139-144.
Hart, G.W. (2006). Sweet insights into learning and memory. Nature chemical biology *2*, 67-68.
Hart, G.W., Housley, M.P., and Slawson, C. (2007). Cycling of O-linked beta-N-acetylglucosamine on nucleocytoplasmic proteins. Nature *446*, 1017-1022.
Hart, G.W., Kreppel, L.K., Comer, F.I., Arnold, C.S., Snow, D.M., Ye, Z., Cheng, X., DellaManna, D., Caine, D.S., Earles, B.J., et al. (1996). O-GlcNAcylation of key nuclear and cytoskeletal proteins: reciprocity with O-phosphorylation and putative roles in protein multimerization. Glycobiology *6*, 711-716.
Hart, G.W., Slawson, C., Ramirez-Correa, G., and Lagerlof, O. (2011). Cross talk between O-GlcNAcylation and phosphorylation: roles in signaling, transcription, and chronic disease. Annual review of biochemistry *80*, 825-858.
Hawkins, M., Angelov, I., Liu, R., Barzilai, N., and Rossetti, L. (1997). The tissue concentration of UDP-N-acetylglucosamine modulates the stimulatory effect of insulin on skeletal muscle glucose uptake. The Journal of biological chemistry *272*, 4889-4895.
Hayes, B.K., and Hart, G.W. (1998). Protein O-GlcNAcylation: potential mechanisms for the regulation of protein function. Adv Exp Med Biol *435*, 85-94.
Herman, M.A., and Kahn, B.B. (2006). Glucose transport and sensing in the maintenance of glucose homeostasis and metabolic harmony. J Clin Invest *116*, 1767-1775.

Ito, R., Katsura, S., Shimada, H., Tsuchiya, H., Hada, M., Okumura, T., Sugawara, A., and Yokoyama, A. (2014). TET3-OGT interaction increases the stability and the presence of OGT in chromatin. Genes Cells *19*, 52-65.
Kao, H.J., Huang, C.H., Bretana, N.A., Lu, C.T., Huang, K.Y., Weng, S.L., and Lee, T.Y. (2015). A two-layered machine learning method to identify protein O-GlcNAcylation sites with O-GlcNAc transferase substrate motifs. BMC Bioinformatics *16 Suppl 18*, S10.
Kent, W.J., Zweig, A.S., Barber, G., Hinrichs, A.S., and Karolchik, D. (2010). BigWig and BigBed: enabling browsing of large distributed datasets. Bioinformatics *26*, 2204-2207.
Li, H. (2018). Minimap2: pairwise alignment for nucleotide sequences. Bioinformatics *34*, 3094-3100.
Li, H., Handsaker, B., Wysoker, A., Fennell, T., Ruan, J., Homer, N., Marth, G., Abecasis, G., Durbin, R., and Genome Project Data Processing, S. (2009). The Sequence Alignment/Map format and SAMtools. Bioinformatics *25*, 2078-2079.
Li, X., Liu, Y., Salz, T., Hansen, K.D., and Feinberg, A. (2016). Whole-genome analysis of the methylome and hydroxymethylome in normal and malignant lung and liver. Genome Res *26*, 1730-1741.
Ling, C., and Ronn, T. (2019). Epigenetics in Human Obesity and Type 2 Diabetes. Cell Metab *29*, 1028-1044.
Lister, R., Pelizzola, M., Dowen, R.H., Hawkins, R.D., Hon, G., Tonti-Filippini, J., Nery, J.R., Lee, L., Ye, Z., Ngo, Q.M., et al. (2009). Human DNA methylomes at base resolution show widespread epigenomic differences. Nature *462*, 315-322.
Loman, N.J., Quick, J., and Simpson, J.T. (2015). A complete bacterial genome assembled de novo using only nanopore sequencing data. Nat Methods *12*, 733-735.
Maresca, A., Zaffagnini, M., Caporali, L., Carelli, V., and Zanna, C. (2015). DNA methyltransferase 1 mutations and mitochondrial pathology: is mtDNA methylated? Front Genet *6*, 90.
Martin, S.E.S., Tan, Z.W., Itkonen, H.M., Duveau, D.Y., Paulo, J.A., Janetzko, J., Boutz, P.L., Tork, L., Moss, F.A., Thomas, C.J., et al. (2018). Structure-Based Evolution of Low Nanomolar O-GlcNAc Transferase Inhibitors. J Am Chem Soc *140*, 13542-13545.
O'Donnell, N., Zachara, N.E., Hart, G.W., and Marth, J.D. (2004). Ogt-dependent X-chromosome-linked protein glycosylation is a requisite modification in somatic cell function and embryo viability. Mol Cell Biol *24*, 1680-1690.
Pertea, M., Pertea, G.M., Antonescu, C.M., Chang, T.C., Mendell, J.T., and Salzberg, S.L. (2015). StringTie enables improved reconstruction of a transcriptome from RNA-seq reads. Nat Biotechnol *33*, 290-295.
Quinlan, A.R., and Hall, I.M. (2010). BEDTools: a flexible suite of utilities for comparing genomic features. Bioinformatics *26*, 841-842.
Ramirez, F., Dundar, F., Diehl, S., Gruning, B.A., and Manke, T. (2014). deepTools: a flexible platform for exploring deep-sequencing data. Nucleic acids research *42*, W187-191.
Ren, W., Gao, L., and Song, J. (2018). Structural Basis of DNMT1 and DNMT3A-Mediated DNA Methylation. Genes (Basel) *9*.
Scott, A., Song, J., Ewing, R., and Wang, Z. (2014). Regulation of protein stability of DNA methyltransferase 1 by post-translational modifications. Acta Biochim Biophys Sin (Shanghai) *46*, 199-203.

Shafi, R., Iyer, S.P., Ellies, L.G., O'Donnell, N., Marek, K.W., Chui, D., Hart, G.W., and Marth, J.D. (2000). The O-GlcNAc transferase gene resides on the X chromosome and is essential for embryonic stem cell viability and mouse ontogeny. Proc Natl Acad Sci U S A *97*, 5735-5739.
Shi, F.T., Kim, H., Lu, W., He, Q., Liu, D., Goodell, M.A., Wan, M., and Songyang, Z. (2013). Ten-eleven translocation 1 (Tet1) is regulated by O-linked N-acetylglucosamine transferase (Ogt) for target gene repression in mouse embryonic stem cells. The Journal of biological chemistry *288*, 20776-20784.
Shin, H., Cha, H.J., Na, K., Lee, M.J., Cho, J.Y., Kim, C.Y., Kim, E.K., Kang, C.M., Kim, H., and Paik, Y.K. (2018). O-GlcNAcylation of the Tumor Suppressor FOXO3 Triggers Aberrant Cancer Cell Growth. Cancer Res *78*, 1214-1224.
Siren, J., Valimaki, N., and Makinen, V. (2014). Indexing Graphs for Path Queries with Applications in Genome Research. IEEE/ACM Trans Comput Biol Bioinform *11*, 375-388.
Slawson, C., Copeland, R.J., and Hart, G.W. (2010). O-GlcNAc signaling: a metabolic link between diabetes and cancer? Trends in biochemical sciences *35*, 547-555.
Thurman, R.E., Day, N., Noble, W.S., and Stamatoyannopoulos, J.A. (2007). Identification of higher-order functional domains in the human ENCODE regions. Genome Res *17*, 917-927.
Torres, C.R., and Hart, G.W. (1984). Topography and polypeptide distribution of terminal N-acetylglucosamine residues on the surfaces of intact lymphocytes. Evidence for O-linked GlcNAc. The Journal of biological chemistry *259*, 3308-3317.
Vasconcelos-Dos-Santos, A., de Queiroz, R.M., da Costa Rodrigues, B., Todeschini, A.R., and Dias, W.B. (2018). Hyperglycemia and aberrant O-GlcNAcylation: contributions to tumor progression. J Bioenerg Biomembr *50*, 175-187.
Walgren, J.L., Vincent, T.S., Schey, K.L., and Buse, M.G. (2003). High glucose and insulin promote O-GlcNAc modification of proteins, including alpha-tubulin. Am J Physiol Endocrinol Metab *284*, E424-434.
Yang, X., and Qian, K. (2017). Protein O-GlcNAcylation: emerging mechanisms and functions. Nature reviews. Molecular cell biology *18*, 452-465.
Yang, Y., Fu, M., Li, M.D., Zhang, K., Zhang, B., Wang, S., Liu, Y., Ni, W., Ong, Q., Mi, J., et al. (2020). O-GlcNAc transferase inhibits visceral fat lipolysis and promotes diet-induced obesity. Nat Commun *11*, 181.
Yang, Y.R., Song, M., Lee, H., Jeon, Y., Choi, E.J., Jang, H.J., Moon, H.Y., Byun, H.Y., Kim, E.K., Kim, D.H., et al. (2012). O-GlcNAcase is essential for embryonic development and maintenance of genomic stability. Aging Cell *11*, 439-448.
Yarychkivska, O., Shahabuddin, Z., Comfort, N., Boulard, M., and Bestor, T.H. (2018). BAH domains and a histone-like motif in DNA methyltransferase 1 (DNMT1) regulate de novo and maintenance methylation in vivo. The Journal of biological chemistry *293*, 19466-19475.
Yompakdee, C., Bun-ya, M., Shikata, K., Ogawa, N., Harashima, S., and Oshima, Y. (1996). A putative new membrane protein, Pho86p, in the inorganic phosphate uptake system of Saccharomyces cerevisiae. Gene *171*, 41-47.
Zhang, Q., Liu, X., Gao, W., Li, P., Hou, J., Li, J., and Wong, J. (2014). Differential regulation of the ten-eleven translocation (TET) family of dioxygenases by O-linked beta-N-acetylglucosamine transferase (OGT). The Journal of biological chemistry *289*, 5986-5996.

Zhou, H., Di Palma, S., Preisinger, C., Peng, M., Polat, A.N., Heck, A.J., and Mohammed, S. (2013). Toward a comprehensive characterization of a human cancer cell phosphoproteome. Journal of proteome research *12*, 260-271.

Zhou, W., Dinh, H.Q., Ramjan, Z., Weisenberger, D.J., Nicolet, C.M., Shen, H., Laird, P.W., and Berman, B.P. (2018). DNA methylation loss in late-replicating domains is linked to mitotic cell division. Nat Genet *50*, 591-602.

Zhou, W., Liang, G., Molloy, P.L., and Jones, P.A. (2020). DNA methylation enables transposable element-driven genome expansion. Proc Natl Acad Sci U S A *117*, 19359-19366.

Graphical abstract

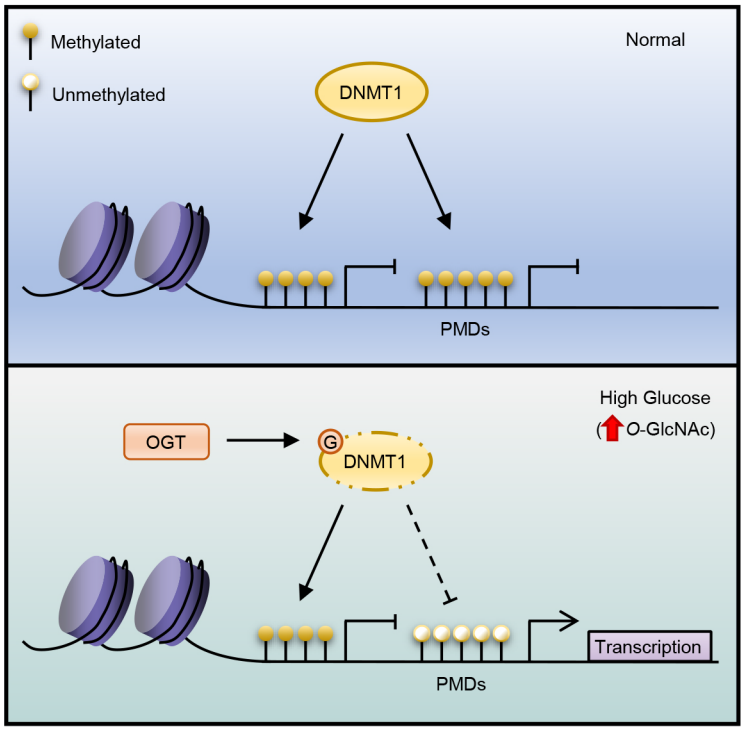

Highlights:

- High glucose increases *O*-GlcNAcylation of DNMT1
- DNMT1 is *O*-GlcNAcylated on S878
- *O*-GlcNAcylation of DNMT1 impairs DNA methyltransferase function
- High glucose reduces DNA methylation at partially methylated domains (PMDs)

MAIN FIGURE TITLES AND LEGENDS

Figure 1. High glucose increases *O*-GlcNAcylation of DNMT1 in cell lines and primary cells.

(A) Hep3B cells were treated glucose or sucrose (5mM or 25mM). Shown are immunoblots of collected lysates using antibody targeting *O*-GlcNAc and GAPDH (n = 3).
(B) Lysates of Hep3B treated with glucose were immunoprecipitated with DNMT1 and immunoprecipitates were immunoblotted with antibody targeting *O*-GlcNAc (n = 3).
(C) PBMCs were isolated from three individual donor blood samples and treated with increasing concentration of glucose for 24 hours. Collected cell lysates from PBMCs were immunoprecipitated with antibody targeting DNMT1 and immunoblotted for *O*-GlcNAc. This is from one donor set. (n = 3).
(D) Pooled PBMCs treated with 25 mM glucose with Thiamet-G were immunoprecipitated with antibody targeting DNMT1 and immunoblotted for *O*-GlcNAc (n = 3).
***$p < 0.0001$ by Student's *t*-test (A-D); n.s., not significant; Data are represented as mean ± SD from three replicates of each sample.

Figure 2. Identification of *O*-GlcNAcylated sites within DNMT1 by LC-MS/MS.

(A) Schematic drawing of the DNMT1 *O*-GlcNAc modified region enriched from Hep3B cells based on mass spectrometry (MS) data and tandem MS (MS/MS) peaks. FTMS + p NSI Full MS [400.0000-1600.0000]. DQDYARFESPPKTQPTEDNKF (S9 HexNAc) – S878.
(B) Schematic diagram of identified novel *O*-GlcNAcylated sites within DNMT1 as determined via MS and OGTsite. DMAP, DNA methyltransferase associated protein-binding domain; PCNA, proliferating cell nuclear antigen-binding domain; NLS, nuclear localization sequences; RFTS, replication foci targeting sequence domain; BAH, bromo-adjacent homology domain.
(C) Each immunoprecipitated Myc-DNMT1 wild type and substituted mutants was immunoblotted with an *O*-GlcNAc antibody (n = 3).

Figure 3. Site specific *O*-GlcNAcylation inhibits DNMT1 methyltransferase function.

For (A)-(D), bar graphs are of relative activity of DNA methyltransferase activity measured as absorbance from of DNMT Activity/Inhibition ELISA easy kit and representative immunoblots of immunoprecipitates performed with antibodies targeting DNMT1.
(A) Hep3B cells were treated 5mM or 25mM glucose with or without TMG (n = 3).
(B) PBMCs from donors were treated with increasing concentrations of glucose (range: 0-20mM) (n = 3).
(C) PBMCs from donors were treated 5mM or 25mM glucose with TMG (n = 3).
(D) Each immunoprecipitated Myc-DNMT1 wild type and substituted mutants were treated with 5mM or 25mM glucose (n = 3).

(E) Each Hep3B and Myc-DNMT1 overexpressed mutants (DNMT1-WT or DNMT1-S878A) were treated 5mM or 25mM glucose or 5-aza (negative control). Shown are absorbance of global DNA methylation of LINE-1 performed with global DNA methylation LINE-1 kit. (n = 3).
*p < 0.001; **p < 0.005; ***p < 0.0001 by Student's t-test (A-E); ns, not significant; Data are represented as mean ± SD from three replicates of each sample.

Figure 4. High glucose leads to loss of DNA methylation at cancer specific partially methylated domains (PMDs).
(A) Density plot of DNA methylation for DNMT1-WT and DNMT1-S878A cells and low or high glucose.
(B) Genome browser screenshot of DNA methylation for DNMT1-WT and DNMT1-S878A cells and low or high glucose along with liver tumor PMDs from (Li et al., 2016).
(C) Boxplots of DNA methylation at PMDs or general genomic background (BG) for each DNMT1-WT and DNMT1-S878A treated with low or high glucose.
(D) Heatmap representation of global DNA methylation for DNMT1-WT and DNMT1-S878A cells under low or high glucose at gene poor and gene rich regions.
(E) Methylation changes from *O*-GlcNAcylation of DNMT1 by wave score for replication timing (Hansen et al., 2010; Thurman et al., 2007).

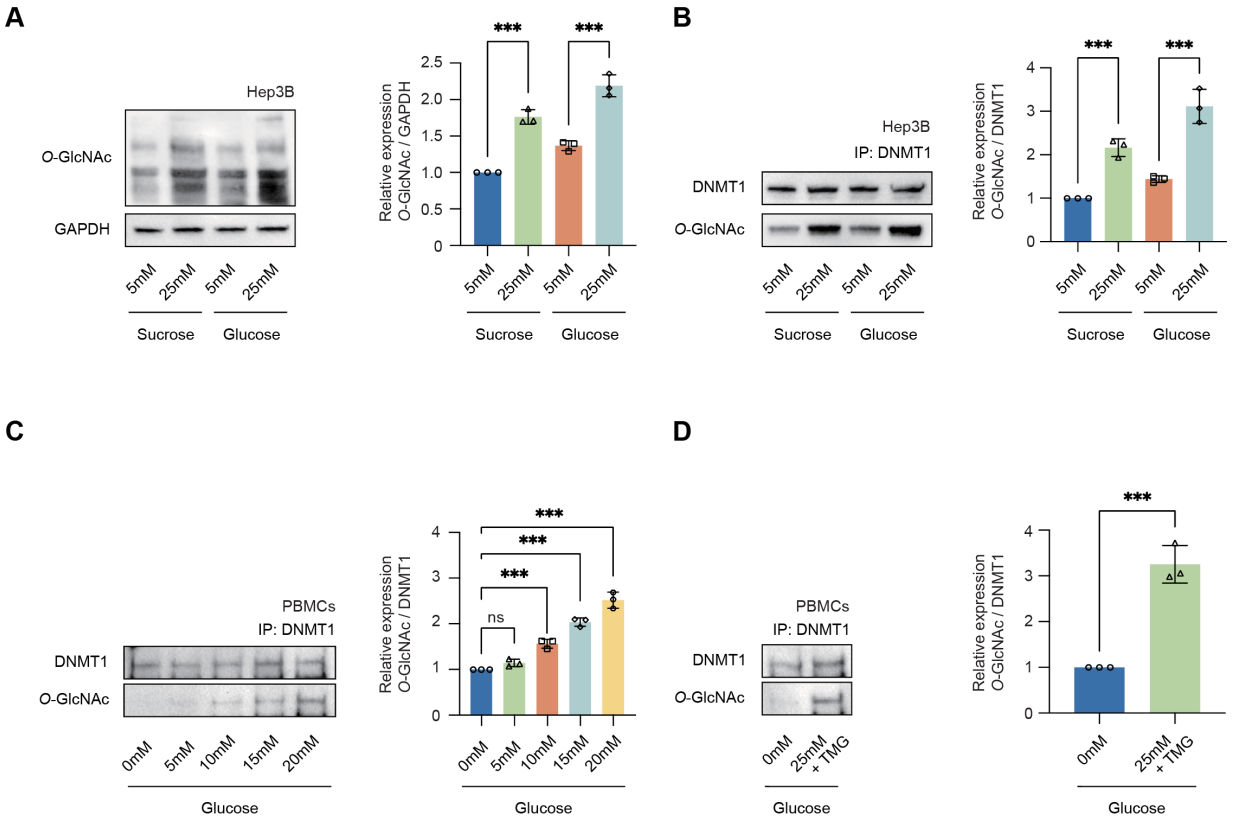

Figure 1. High glucose increases *O*-GlcNAcylation of DNMT1 in cell lines and primary cells.

(A) Hep3B cells were treated glucose or sucrose (5mM or 25mM). Shown are immunoblots of collected lysates using antibody targeting *O*-GlcNAc and GAPDH (n = 3).

(B) Lysates of Hep3B treated with glucose were immunoprecipitated with DNMT1 and immunoprecipitates were immunoblotted with antibody targeting *O*-GlcNAc (n = 3).

(C) PBMCs were isolated from three individual donor blood samples and treated with increasing concentration of glucose for 24 hours. Collected cell lysates from PBMCs were immunoprecipitated with antibody targeting DNMT1 and immunoblotted for *O*-GlcNAc. This is from one donor set. (n = 3).

(D) Pooled PBMCs treated with 25 mM glucose with Thiamet-G were immunoprecipitated with antibody targeting DNMT1 and immunoblotted for *O*-GlcNAc (n = 3).

***$p < 0.0001$ by Student's *t*-test (A-D); n.s., not significant; Data are represented as mean ± SD from three replicates of each sample.

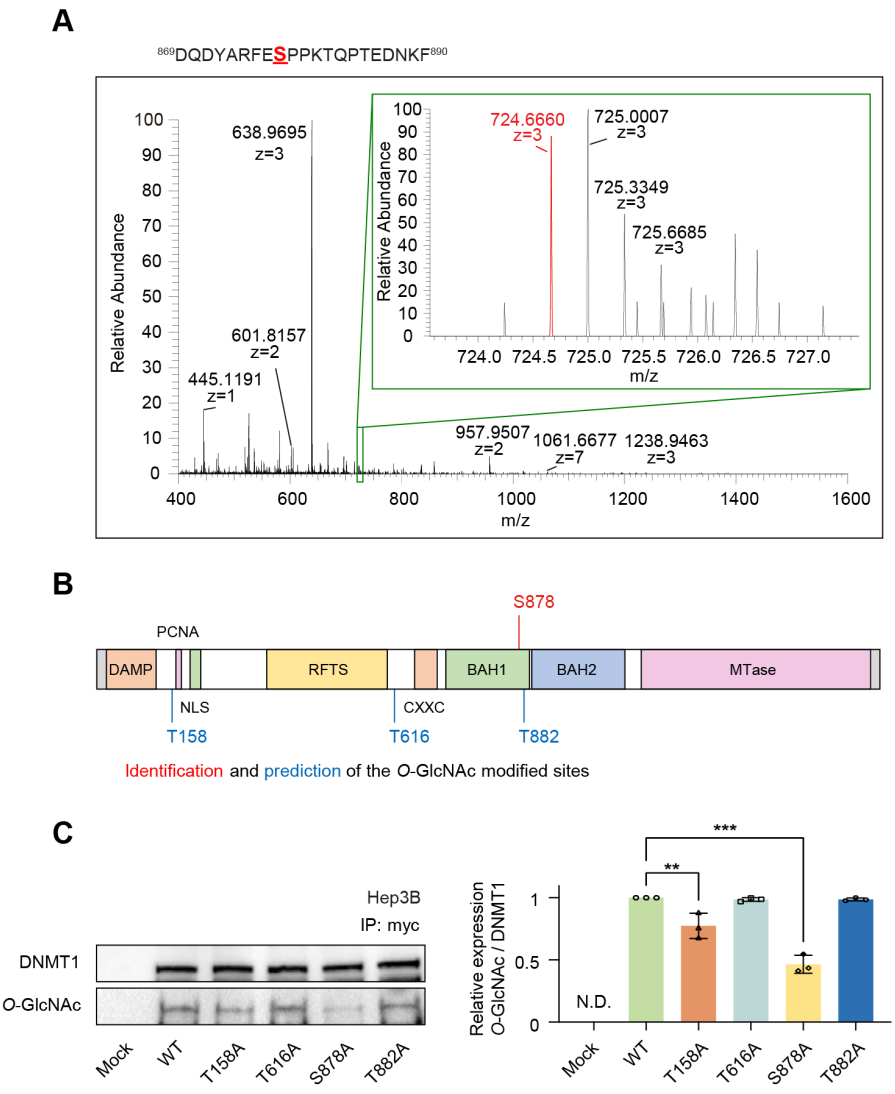

Figure 2. Identification of *O*-GlcNAcylated sites within DNMT1 by LC-MS/MS.

(A) Schematic drawing of the DNMT1 *O*-GlcNAc modified region enriched from Hep3B cells based on mass spectrometry (MS) data and tandem MS (MS/MS) peaks. FTMS + p NSI Full MS [400.0000-1600.0000]. DQDYARFESPPKTQPTEDNKF (S9 HexNAc) – S878.

(B) Schematic diagram of identified novel *O*-GlcNAcylated sites within DNMT1 as determined via MS and OGTsite. DMAP, DNA methyltransferase associated protein-binding domain; PCNA, proliferating cell nuclear antigen-binding domain; NLS, nuclear localization sequences; RFTS, replication foci targeting sequence domain; BAH, bromo-adjacent homology domain.

(C) Each immunoprecipitated Myc-DNMT1 wild type and substituted mutants was immunoblotted with an *O*-GlcNAc antibody (n = 3).

$^{**}p < 0.005$; $^{***}p < 0.0001$ by Student's *t*-test (C); N.D., not detected; Data are represented as mean ± SD from three replicates of each sample.

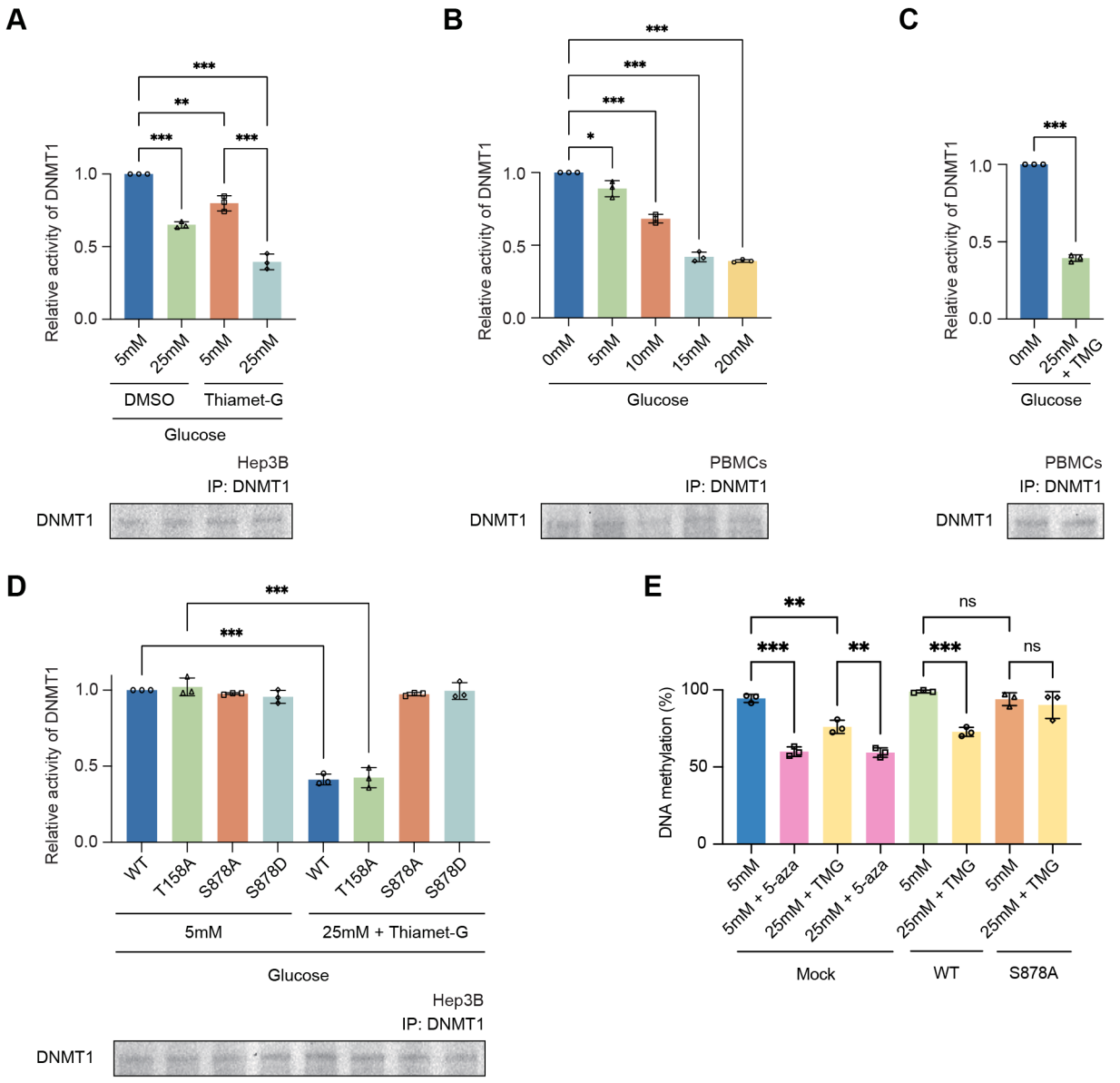

Figure 3. Site specific *O*-GlcNAcylation inhibits DNMT1 methyltransferase function.
For (A)-(D), bar graphs are of relative activity of DNA methyltransferase activity measured as absorbance from of DNMT Activity/Inhibition ELISA easy kit and representative immunoblots of immunoprecipitates performed with antibodies targeting DNMT1.
(A) Hep3B cells were treated 5mM or 25mM glucose with or without TMG (n = 3).
(B) PBMCs from donors were treated with increasing concentrations of glucose (range: 0-20mM) (n = 3).
(C) PBMCs from donors were treated 5mM or 25mM glucose with TMG (n = 3).
(D) Each immunoprecipitated Myc-DNMT1 wild type and substituted mutants were treated with 5mM or 25mM glucose (n = 3).

(E) Each Hep3B and Myc-DNMT1 overexpressed mutants (DNMT1-WT or DNMT1-S878A) were treated 5mM or 25mM glucose or 5-aza (negative control). Shown are absorbance of global DNA methylation of LINE-1 performed with global DNA methylation LINE-1 kit. (n = 3).

*p < 0.001; **p < 0.005; ***p < 0.0001 by Student's t-test (A-E); ns, not significant; Data are represented as mean ± SD from three replicates of each sample.

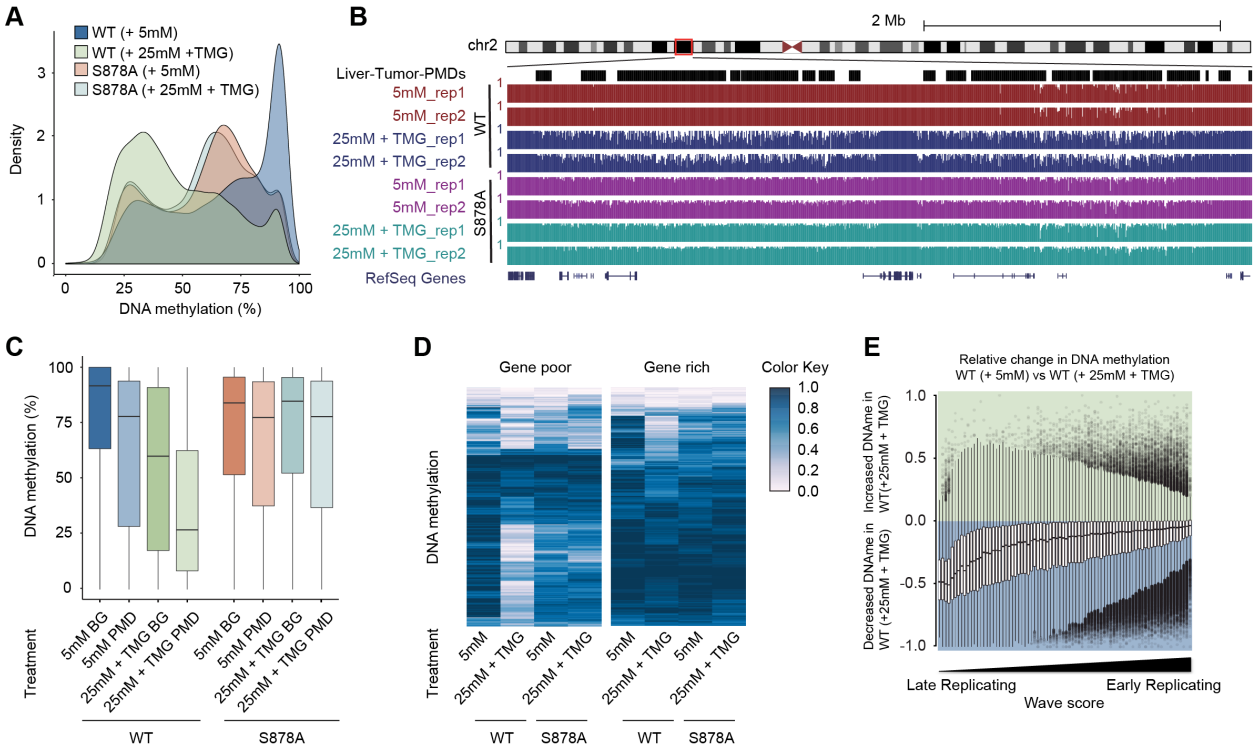

Figure 4. High glucose leads to loss of DNA methylation at cancer specific partially methylated domains (PMDs).

(A) Density plot of DNA methylation for DNMT1-WT and DNMT1-S878A cells and low or high glucose.

(B) Genome browser screenshot of DNA methylation for DNMT1-WT and DNMT1-S878A cells and low or high glucose along with liver tumor PMDs from (Li et al., 2016).

(C) Boxplots of DNA methylation at PMDs or general genomic background (BG) for each DNMT1-WT and DNMT1-S878A treated with low or high glucose.

(D) Heatmap representation of global DNA methylation for DNMT1-WT and DNMT1-S878A cells under low or high glucose at gene poor and gene rich regions.

(E) Methylation changes from *O*-GlcNAcylation of DNMT1 by wave score for replication timing (Hansen et al., 2010; Thurman et al., 2007).